

PACS numbers: 85.60.Jb; 42.55.Px; 42.30.Wb
DOI: 10.1070/QE2004v034n10ABEH002799

Broadband light source based on quantum-well superluminescent diodes for high-resolution optical coherence tomography

D.S. Adler, T.H. Ko, A.K. Konorev, D.S. Mamedov,
V.V. Prokhorov, J.J. Fujimoto, S.D. Yakubovich

***Abstract*. Emission of single quantum-well superluminescent diodes of two types in spectral ranges between 810 and 870 nm and between 860 and 970 nm is combined with the help of an original broadband fibre Y-coupler. Such a light source produces more than 5 mW of the cw output optical power and has a record small coherence length of about 5 μm. Its relative intensity noise does not exceed −135 dB Hz^{-1} in the 100-kHz – 10-MHz frequency range. The use of this source in an optical coherence tomography provides the recording of tomograms of biological objects *in vivo* with a spatial resolution of 2 – 3 μm.**

Keywords: *superluminescent diode, broadband fibre coupler, optical coherence tomography*.

1. Introduction

Optical coherence tomography (OCT) is a method allowing the two-dimensional imaging of biological tissue sections with a high spatial resolution *in vivo* [1, 2]. The main requirements imposed on light sources for OCT is a high brightness and a low degree of coherence. Standard OCT methods with the 10 – 15-μm spatial resolution are widely used in various fields of medical diagnostics. Recently [3, 4], an axial resolution of 1 – 3 μm was achieved in OCT using a femtosecond solid-state laser. However, such systems are too bulky, inconvenient in operation, and quite costly, which severely impedes their clinical applications.

The advantages of semiconductor light sources are well known. These are high efficiency, small size, high reliability, simplicity of integration into electronic and optoelectronic circuits, and low cost of mass production. The optimal light sources for OCT are light-emitting modules based on superluminescent diodes (SLDs), which have a high brightness and a small coherence length $L_c = \lambda^2/\Delta\lambda$, where λ is the wavelength of light and $\Delta\lambda$ is the emission spectral width.

A.K. Konorev, D.S. Mamedov, V.V. Prokhorov Superluminescent Diodes Limited Liability Company, Box 70, B-454, 119454 Moscow, Russia;
S.D. Yakubovich Moscow State Institute of Radio Engineering, Electronics, and Automatics (Technical University), prosp. Vernadskogo 78, 119454 Moscow, Russia;
D.C. Adler, T.H. Ko, J.G. Fujimoto Department of Electrical Engineering and Computer Science, Research Laboratory of Electronics, Massachusetts Institute of Technology, Cambridge, MA 02139, USA

Received 13 May 2004
Kvantovaya Elektronika **34** (10) 915 – 918 (2004)
Translated by M.N. Sapozhnikov

The broadest-band commercial SLDs emitting in the near-IR range between 750 and 1000 nm have the coherence length $L_c = 12 - 15$ μm. To our knowledge the record coherence length $L_c = 7$ μm was achieved in Refs [5, 6] (the median wavelength was $\lambda_m = 825$ nm and $\Delta\lambda = 98$ nm) for a SLD based on a single (GaAl)As quantum-well heterostructure (SQW). However, this result was obtained using combined pulsed-continuous injection, and therefore the average output power coupled out through a single-mode fibre (SMF) was low (0.2 mW).

It is obvious that the emission band can be expanded and the degree of coherence lowered by using combined light sources providing the superposition of emission of two or more SLDs with shifted but overlapped emission bands. Such a superposition can be achieved in SLD modules with output SMFs by using broadband fibre couplers.

2. Spectral parameters of the SLD

A combined broadband light source used in our study was manufactured from quantum-well SLDs of two types: (GaAl)As single quantum-well SLDs with a step waveguide, similar to those described in Refs [5, 6] and emitting in the 810 – 870-nm spectral range (type I) and recently developed (InGa)As/(AlGa)As single quantum-well SLDs with a gradient waveguide [7] emitting in the 860 – 970-nm spectral range (type II). SLDs of both types had a conventional design [7].

A continuous spatially homogeneous injection was used. The output emission spectra exhibited two maxima of the intensity I corresponding to quantum transitions from different quantum subbands. The dependence of the spectra on the injection current J is shown in Fig. 1. For low injection currents, only the long-wavelength maximum is observed. As the current increases, the short-wavelength maximum appears which grows faster than the long-wavelength one. The intensities of these maxima become equal at some current (the corresponding spectrum is shown by a thick curve). As the injection current further increases, the short-wavelength maximum dominates.

As the active-channel length L_a is increased, the levelling of the spectral maxima is achieved at a higher current and a higher output power; however, the maxima become narrower and the dip between them becomes deeper.

The operating regimes of SLDs providing the levelled spectral maxima are most convenient for the development of a combined broadband light source. In this case, the SLD optimisation is reduced to the determination of the value of L_a for each type of the SLDs, which provides a sufficiently

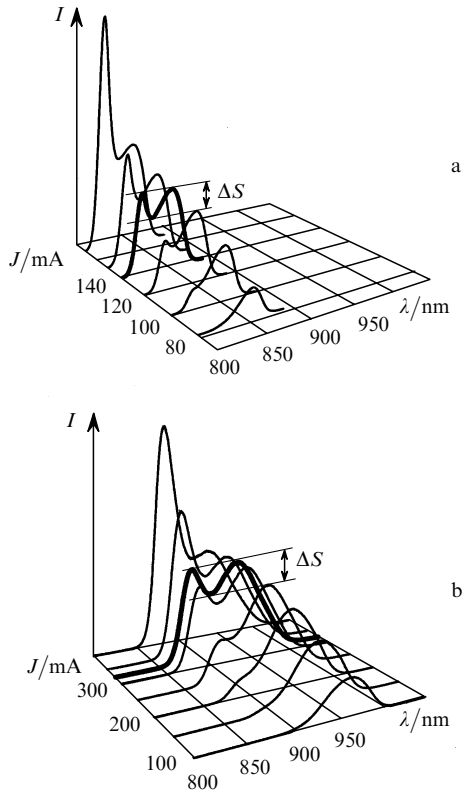

Figure 1. Dependences of the output emission spectra of quantum-well (GaAl)As (a) and (InGaAl)As (b) SLDs on the injection current (ΔS is the spectral dip).

high output power, the acceptable dip in the spectral curve with equalised maxima, and the approximate equality of the spectral intensity densities in the superposition (taking the transfer characteristics of a fibre coupler into account). When symmetric X- or Y-couplers are used, the output powers of the SLDs should be directly proportional to the widths of their spectral bands.

The widths of the emission bands of SLDs of types I and II with equalised spectral maxima were ~ 50 and 100 nm, respectively. The requirements formulated above were fulfilled by using the active channel lengths $L_a^I = 1400$ μm and $L_a^{II} = 800$ μm. In this case, the SLD modules of types I and II produced the output powers $P_{sm}^I \approx 3.6$ mW and $P_{sm}^{II} \approx 7.2$ mW at the SMF output. An additional degree of freedom allowing the tuning of emission bands during their 'joining' is the SLD operation temperature. The central wavelength of the SLD emission band shifts to the red with increasing temperature with the rate of ~ 0.4 nm K^{-1}.

3. Combined light source

SLDs described above were mounted on thermoelectric microcoolers in standard DIL packages. Temperature sensors (thermistors) were mounted in heat conductors of the modules. The SLD emission was coupled out through isotropic Corning Pure Mode HI 780 SMFs with microlenses for efficient coupling. Currents determining the operation regime and thermal stabilisation were provided by a Pilot-4 two-channel current–temperature controller.

The original element of the light source is a broadband Y-coupler based on the SMF of the type considered above, which was developed within the framework of this study. It is known that commercial single-mode spliced fibreoptic couplers for the near-IR range have an acceptably constant coupling ratio only in a rather narrow spectral band and therefore cannot be used in the light source considered here. The scheme of the developed Y-coupler is presented in Fig. 2. The SMF ends with AR coatings were fixed with an identical displacement relative to the optical axis of the coupler. As collimators, gradient (Fig. 2a) or garnet ball (Fig. 2b) microlenses were used. In the second case, a beamsplitter was a plane–parallel plate with one of the faces covered by an AR coating and the other one having a dielectric coating containing alternating Si and SiO_2 layers providing the reflectivity close to 50 % in the 750–1050-nm spectral range (Fig. 2c). In this case, the excess optical insertion loss did not exceed 1 dB.

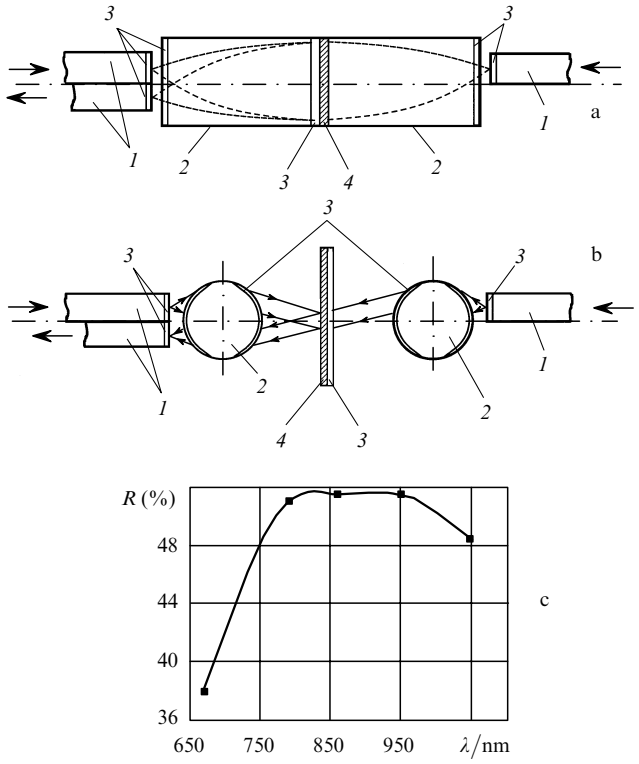

Figure 2. Schemes of a broadband fibre Y-coupler with collimators based on gradient (a) and ball (b) microlenses and the spectral dependence of the reflectivity R for a multilayer translucent coating (c): (*1*) optical fibres; (*2*) microlenses; (*3*) multilayer AR coatings; (*4*) multilayer semireflecting coating.

The basic output characteristics of the combined light source at the operating point corresponding to the equalised spectral maxima and the 5.2-mW power at the Y-coupler output are presented in Fig. 3. The output emission spectrum (Fig. 3a) has the central wavelength at 890 nm and the FWHM $\Delta\lambda = 152$ nm, corresponding to the coherence length $L_c = 4.6$ μm. The corresponding coherence function of the intensity is shown in Fig. 3b. The radio-frequency spectrum of the relative intensity noise (RIN) is presented in Fig. 3c. Circuits used in a Pilot-4 controller to stabilise the current insures the RIN at a level of less than -135 dB Hz^{-1} in the typical 10-kHz–30-MHz OCT band. Such a RIN level, which noticeably exceeds the shot noise, is typical for

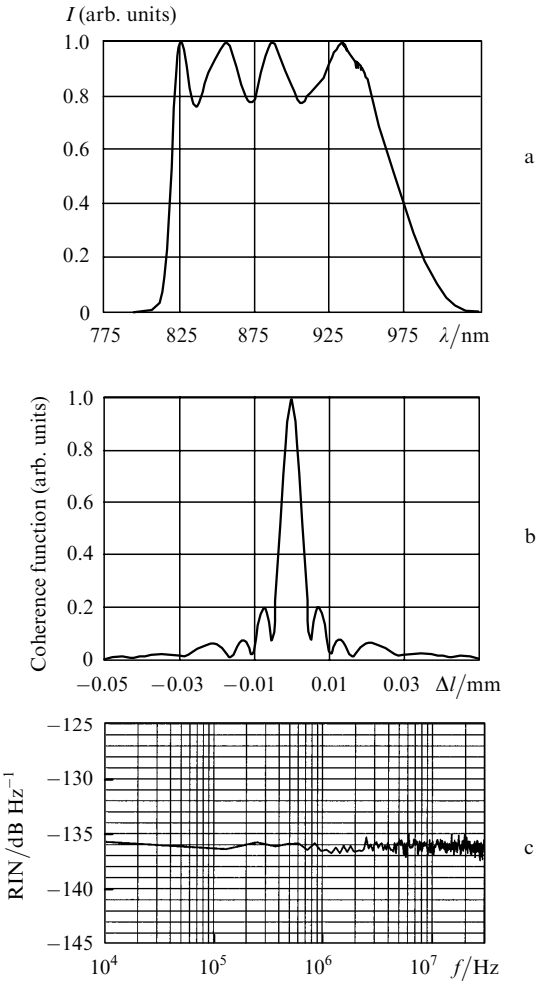

Figure 3. Output emission spectrum (a), coherence function (b), and RIN spectrum (c) of a combined SLD light source (Δl is the optical path difference).

the internal (quantum) noise of SLDs [8] and is considerably lower than in alternative light sources used in OCT.

4. Use of the broadband light source in OCT

The combined light source described above was used in an optical coherence tomograph whose scheme is presented in Fig. 4. A sufficiently low RIN level allowed us to abandon a scheme of double balance detection, which is conventionally used in high-resolution OCT, and employ only one photodetector, which significantly simplified the system. Figure 5 shows the images of a human eye retina obtained with the help of our system using the combined light source based on SLDs (Fig. 5a), a mode-locked Ti : sapphire laser (with a double balance photodetection circuit (Fig. 5b), and a commercial light-emitting SLD module emitting at 830 nm (Fig. 5c). Analysis of these images shows that the 3.2-μm axial resolution achieved with the help of the combined source is close to that obtained using a femtosecond laser, which allows us to visualise qualitatively the morphological structure of retina tissues, a layer of nerve fibres, a layer of nerve-knot cells and a photoreceptor layer. The standard OCT method (Fig. 5c) cannot provide the axial resolution sufficient for this.

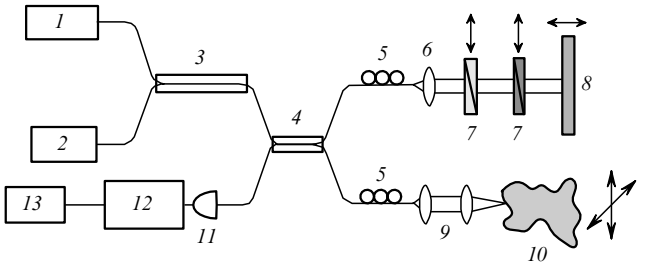

Figure 4. Scheme of the optical coherence tomograph: (*1*) SLD module of type I; (*2*) SLD module of type II; (*3*) broadband Y-coupler; (*4*) broadband X-coupler; (*5*) polarisation controller; (*6*) collimator; (*7*) compensator; (*8*) reference mirror; (*9*) microscope; (*10*) biological object; (*11*) photodetector; (*12*) band amplifier – demodulator; (*13*) PC.

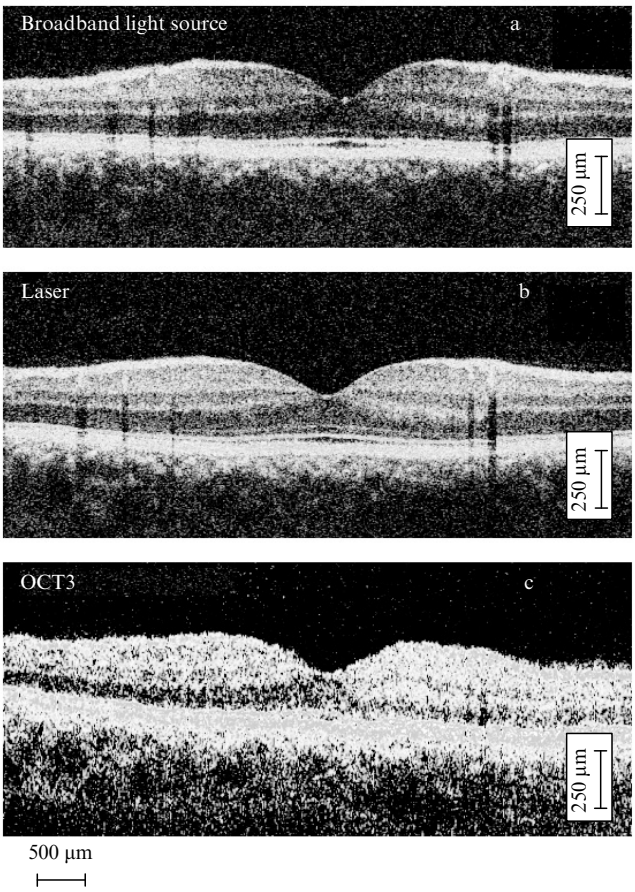

Figure 5. Tomograms of a human-eye retina recorded using a combined SLD light source (a), Ti : sapphire femtosecond laser (b), and commercial OCT3 SLD module (c).

This system was used to study various pathologies of the eye retina *in vivo* for many patients, namely, holes in the yellow spot, yellow spot's edema, diabetic retinopathy, age yellow-spot degeneration, epiretinal membrane, central serum chorioretinopathy, pigment degeneration of retina and glaucoma [9, 10].

Unfortunately, the spectral position of the emission band of this combined source is not optimal for ophthalmology because the eye fluid consisting mainly of water absorbs the long-wavelength wing of the emission spectrum. Figure 6 shows the transmission spectra of aqueous layers in the near-IR region [11]. The estimate shows that during

OCT of the human eye retina about 30 % of the emission energy of the combined source is not used, and the effective coherence length increases approximately by the same factor. The use of this system for OCT of skin layers provided the 2.3-μm axial resolution.

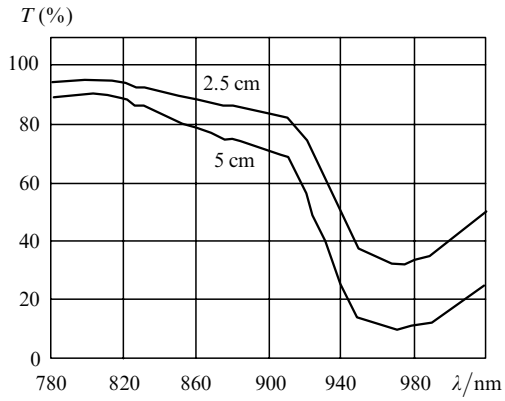

Figure 6. Transmission spectra of 2.5-cm and 5-cm thick aqueous layers.

5. Conclusions

We have built a combined light source in which emission from two quantum-well SLDs emitting in the 810 – 870-nm and 860 – 970-nm bands is combined with the help of a broadband fibre coupler. The width of the output emission band exceeds 150 nm and the coherence length is about 5 μm. The use of this source in optical coherence tomography provided the axial resolution of 2.3 – 3.2 μm in analysis of various biological objects. This is very important for medical diagnostics, considerably simplifying coherence tomographs and reducing their cost. Of great interest for ophthalmologic diagnostics is the development of a similar light source emitting in the spectral region shifted by 50 – 60 nm to the blue.

Acknowledgements. This work was partially supported by Contracts R01-EY11289-16, R01-EY13178, P30-EY13078 (NIH); ECS-0119452 (NSF); F49620-98-1-0139 (AFOSR); F49620-01-1-0186, FWFP14218-PSY, FWFV159-PAT, CRAF-1999-70549 (MFELP); Grant No 26151P (ISTC), and by Carl Zeiss Meditec Company. The authors thank A.T. Semenov for his attention to this work and S.P. Orobinsky for assembling fibre couplers.

References

1. Huang D., Swanson E.A., Lin C.P., Shuman J.S., Stinson W.G., Chang W., Hee M.R., Flotte T., Gregory K., Puliafito C.A., Fujimoto J.G. *Science*, **254**, 1178 (1991).
2. Fercher A.F., Drexler W., Hitzenberger C.K., Lasser T. *Rep. Prog. Phys.*, **66**, 293 (2003).
3. Drexler W., Morgner U., Ghanta R.K., Kaertner F.X., Shuman J.S., Fujimoto J.G. *Nature Medicine*, **7**, 502 (2001).
4. Drexler W., Sattmann H., Hermann B., Ko T.H., Stur M., Unterhuber A., Scholda C., Wirtitsch M., Fujimoto J.G., Fercher A.F. *Archives of Ophthalmology*, **121**, 695 (2003).
5. Semenov A.T., Batovrin V.K., Garmash I.A., Shidlovski V.R., Shramenko M.V., Yakubovich S.D. *Electron. Lett.*, **31** (4), 314 (1995).
6. Batovrin V.K., Garmash I.A., Gelikonov V.M., Gelikonov G.V., Lyubarskii A.V., Plyavenek A.G., Safin S.A., Semenov A.T., Shidlovskii V.R., Shramenko M.V., Yakubovich S.D. *Kvantovaya Elektron.*, **23**, 113 (1996) [*Quantum Electron.*, **26**, 109 (1996)].
7. Mamedov D.S., Prokhorov V.V., Yakubovich S.D. *Kvantovaya Elektron.*, **33**, 471 (2003) [*Quantum Electron.*, **33**, 471 (2003)].
8. Yurek A.M., Taylor H.F., Goldberg L., Weller J.F., Dandridge A. *IEEE J. Quantum Electron.*, **22** (4), 522 (1986).
9. Adler D.C., Ko T.H., Mamedov D., Prokhorov V., Shidlovski V., Yakubovich S., Fujimoto J.G. *Tech. Digest on Conf. «OSA Biomedical Topical Meeting» (BIOMED 2004)* (Miami Beach, Fla, USA, 2004) SE2 Paper.
10. Fujimoto J.G., Ko T.H., Adler D.C., Mamedov D., Prokhorov V., Shidlovski V., Yakubovich S., Woitkovski M.D., Duker J.S., Shuman J.S. *Tech. Digest on Conf. «Association for Research in Vision and Ophthalmology» (ARVO 2004)* (Ford Lauderdale, Fla, USA, 2004, ARVO Presentation Listing 3002/B637).
11. Hale G.M., Querry M.R. *Appl. Opt.*, **12**, 555 (1973).